Indian Journal of Chemical Technology
Vol. 24, May 2017, pp. 344-351

Investigation of the effects of various parameters on mixing time in pilot stirred tank equipped single and dual rushton impeller

Firuz Fakheri*,[1], Jafarsadegh Moghaddas[2], Sajjad Fereidoni[3] & Hossein Attar[3]

[1]Member of Young Researchers and Elite Club, Islamic Azad University, Science and Research Branch, Tehran, Iran
[2]Transport Phenomena Research Center, Chemical Engineering Faculty, Sahand University of Technology, P.O. Box 51335/1996, Tabriz, Iran
[3] Islamic Azad University, Pharmaceutical Sciences Branch, Tehran, Iran.
E-mail: eng.fakheri@gmail.com

Received 25 October 2015; accepted 15 March 2016

The optimum positions for the additive injection and probe location in a dual-Rushton stirred tank have been investigated using Response Surface Methodology. Therefore, by keeping these two parameters (probe location and additive injection point) fixed during consequent experiments, the single Rushton impeller has been compared with a dual Rushton impeller stirred tank. The results have shown that the mixing time for single impeller systems, is lower than that for double impeller systems, so to obtain a lower mixing time in multi impeller systems, it is necessary to obtain the relation between the height of the liquid and the number of impellers. In the next part, the obtained mixing time is compared against simulation results and published data based on experimental works for a Rushton impeller in different configurations of a vessel. Also in this work the effects of superficial gas velocity and impeller rotational speed for both systems have been investigated.

Keywords: Stirred tank, Mixing time, RSM, Rushton turbine, Aeration

The mixing or agitation of liquids in stirred tanks are widely used in the process industries and one of the most important unit in the many industries such as chemical, food, oil and petrochemical processing for mixing single or multiphase fluids. Now a days, this type of system is very suitable for the solid-liquid-gas dispersion in the liquid, with or without chemical reaction[1,2].

In many situations, mixing time is an important factor to optimize mixing tank design with single and multiple impellers[3]. In fact, the product quality and production costs are affected by optimization of stirred tank design. Mixing time can be used as a comparative factor of the mixers efficiency, with the same power input[2,4].

The ideal geometry of the helical mixing systems (pitch size ratio, clearance-wall, blade width, number of blades) has been investigated by Delaplace *et al.*[5] and they showed that the global mixing characteristics of a helical ribbon mixer are independent of Re for a laminar flow. The studies on mixing time have been carried out using acid/base/indicator reaction, temperature variation, planar laser-induced fluorescence (PLIF) technique and conductivity technique. The results obtained for mixing time by researchers is different because the mixing time is dependent on the type of mixing process, the geometrics of the system, the definition and method of measurement of the system[5]. A comparison of the two types of methods has previously been reported by researchers.

Chomcharn[6] has compared between physical (conductivity probe technique) and colorimetric methods for the unbaffled system and have indicated that the colorimetric method produces results that were in agreement with the conductivity method only when two probes are used. Paglianti and Pintus[7] showed that mixing time measured in chemically reacting system were, on average, 22% shorter than the values measured using the conductivity technique. In order to mixing times comparison the measuring method must be the same in all experiments.

Gas-liquid mixing time measurements in several techniques are different, this difference may be due to the geometrics of the impeller, the probe location, the tracer injection point and the process condition and measurement techniques. Thus, there are few studies for mixing time under aerated conditions.

Otomo *et al.*[8] measured the unaerated and aerated mixing time by improvement on a conductivity method. They found that the influence of gas flow rate on the mixing time was not significant. Pandit and Joshi[9] investigated mixing times under aerated conditions using *p*H and conductivity probe. They showed that the mixing times increased with an increase in the gas flow rate, but decreased under flooding rates and, among the data obtained by both techniques, there was no significant difference.

The parameters affecting the mixing time in a fixed geometrical condition in present study are: the

impellers rotational speed N, superficial gas velocity v_s, point of bulk injection tracer and conductivity probe location. For each experiment, a pulse of electrolyte is added to the liquid bulk and the mixing time required to achieve 95% of the final concentration of the tracer is measured by conductometer (t_{95})[10].

In this work, two types of stirred tank systems for determining the mixing time were used, i) the first sets of experiments were carried out in the stirred tank equipped with a single Rushton turbine and ii) the second sets of experiments were carried out in a Double-Rushton stirred tank. The mixing time obtained from these two mixing systems has also been compared with the previous works.

The objective of this work is the optimization of the probe location and the injection point in order to experimentally compare the liquid and gas-liquid mixing time of these two types of systems as well as with previous works, and finally, to obtain the relationship between the heights of the liquids in these two systems of stirred tank for measuring low mixing times. The optimization of these parameters requires many tests, which is time consuming and exorbitant in cost. In order to overcome this problem, the optimization of these parameters has been carried out using multivariate statistic techniques. Now a days, experimental design methods, such as the factorial design, response surface methodology (RSM) and Taguchi methods are widely used for the optimization of response surface[11,12]. In this work, response surface methodology (RSM) is used to find a reasonable approximation for the functional relationship between a response variable and independent variables.

Theory

Response Surface Methodology

For the variables measurable, the response surface can be expressed as follows:[11]

$$Y = f(x_1, x_2, \ldots, x_n) \quad \ldots (1)$$

The goal is to optimize the response variable, Y (mixing time) and x_i, the independent variables of called factors. The design consists of factorial design points with 2^k runs, 2k axial or star points, and n replications at the center of the design[11,13]. The correlation of the independent variables and the response were estimated by a second-order polynomial Eq. 2 and is expressed as[14]:

$$\hat{Y}_i = \beta_0 + \sum_{i=1}^{k} \beta_i x_i + \sum_{i=1}^{k} \sum_{j=2}^{k} \beta_{ij} x_i x_j + \sum_{i=1}^{k} \beta_{ii} x_i^2 + e = \beta_0 + x_i' \beta + x_i' \beta x_i + e_{ij} \quad \ldots (2)$$

where $\hat{Y}_i$ is the mixing time, β_0 is the value of fitted response at the center point of the design, e the residual (error) term, β_i, β_{ii} and β_{ij} are the linear, quadratic and interaction terms respectively, and x_i the dimensionless coded variables.

Codification of the levels of the variable

According to the Equation below, it can be used to transform a real value (X_i) into a dimensionless coded value (x_i)[15]:

$$x_i = \left(\frac{X_i - X_0}{\Delta X_i} \right) \qquad i = 1,2,3,\ldots,k \quad \ldots (3)$$

where x_i is the dimensionless coded value; X_i is the real value; X_0 is the real value at the center point and ΔX_i is the step change.

According to the Eq. 2, the quadratic model including linear, squared and interaction terms. The importance of terms in the model by analysis of variance (ANOVA) are characterized[13].

Experimental Section

Instrumentation and equipment

The experimental setup is shown schematically in Fig. 1.

All experiments were carried out in a transparent vessel with a flat bottom, having an inner diameter, T, of 0.3 m. The cylindrical tank body was made of glass and the working heights liquid were 0.54 m (first tank) and 0.3 m (second tank). The stirred tank was fitted with four wall mounted baffles having a width of 1/10th and thickness 1/100th that of the tank diameter (fully baffled condition). In the first system, two six – bladed Rushton turbine impellers and in the second system, a six-bladed Rushton turbine with a diameter of D = T/3 were mounted on the shaft. The impeller width, L, and the impeller blade height, W, were equal to D/4 and D/5. The off – bottom clearance is C1 = 0.55T, and the upper impeller is placed ΔC = 0.7T above the lower one. An aeration gas was introduced 5 cm under the bottom impeller through a perforated plate distributor having a 7.5 cm diameter and 31 orifices.

The stirred tank is filled with tap water as the main continuous phase fluid, whose surface distances from the upper impeller was C2 = 0.55T. A pump drives the

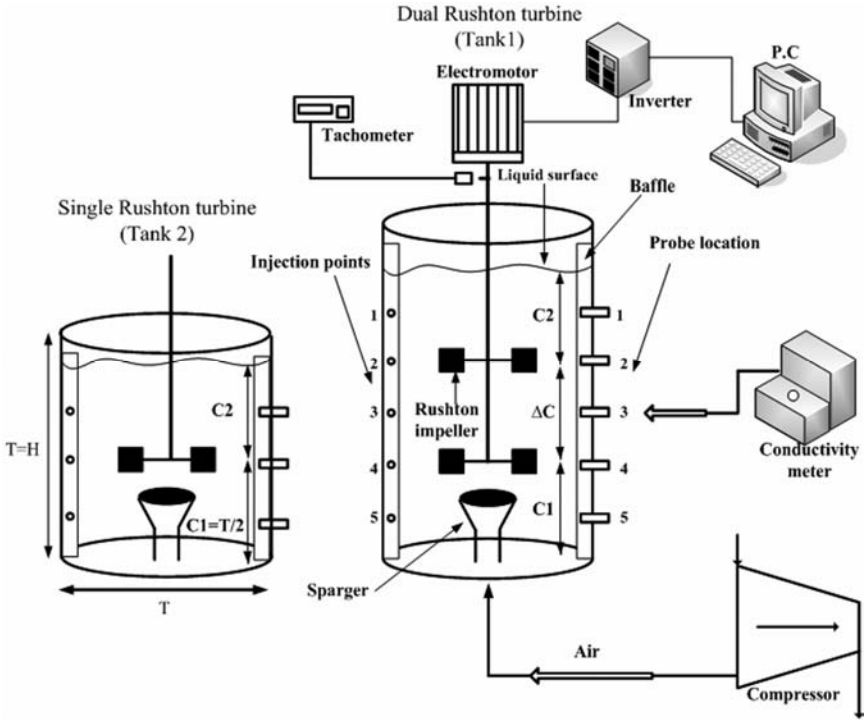

Fig. 1 — Schematic of the experimental set with details of the tanks.

turbines and the stirring speed is measured using a calibrated digital oscilloscope. A tachometer was used to measure the impeller speed. A pulse of 50 mL of NaCl solution (120 g/L) per 3 second has been injected at axial distances in the tank wall and five ports were used for tracer detection. The position of the probe and the tracer injection point were situated in across to each other in the state of an axially parallel. The mixing time was estimated for each of the probes as the time required to attain 95% of the final concentration within ±5% of the average concentration.

Conductivity probe technique

In exactly the same experimental conditions, conductometer probe response at different measurement locations was normalized to the same overall concentration change. The variance can be expressed as follows:[16]

$$\sigma^2 = \frac{1}{5}\sum_{i=1}^{5}(C_i'(t)-1)^2 \quad \ldots (4)$$

where i is the number of probe, for one probe $\sigma^2 = (C'(t)-1)^2$

and:

$$C'(t) = \frac{C(t)-C_0}{C(\infty)-C_0} = \frac{C(t)}{C(\infty)} \quad \ldots (5)$$

Table 1 — Experimental range and levels of the independent variable

Impellers rotational speed (rpm)		Superficial gas velocity (mm/s)		Probe location		Tracer injection point	
Real value X_1	Coded value x_1	Real value X_2	Coded value x_2	Real value X_3	Coded value x_3	Real value X_4	Coded value x_4
600	2	2.29	2	5	2	5	2
500	1	1.81	1	4	1	4	1
400	0	1.35	0	3	0	3	0
300	-1	0.87	-1	2	-1	2	-1
200	-2	0.40	-2	1	-2	1	-2

where C′(t) is the value of the normalized response at time t. According to the Eq. 4 the obtained mixing time by using variance gives overall mixing time[16-18]. The mixing time is reached when the final concentration fluctuation crosses the line Log (σ^2) = -2.6[17].

Experimental design

'MINITAB' software (a package from Minitab Inc.) statistical package used in this paper for calculation and analysis of the second order polynomial coefficients. The levels chosen for the independent variables, impellers rotational speed (x_1), superficial gas velocity (x_2), probe location (x_3) and tracer injection point (x_4) were shown in Table 1. Central composite rotatable design (CCRD) of the experiments was used, where the values of

independent variables were coded as the variables, x, in the range of +2 and - 2 levels.

This design was composed of a 2^4 factorial design (runs 1–16), 8 star points (runs 17–24) and 6 replicates (runs 25–30), thus 30 experiments were needed in total. The mean value of the response (mixing time) obtained in 30 experiments are summarized in Table 2.

The experimental data were analyzed using central composite rotatable design to predict the mixing time (see Table 2). In order to estimate the curvature and experimental error of the model, the star points and the replicates were added to experimental design[19].

According to Eq. 3, the relations between the coded and the central value were as given below:

$$x_1 = (X_1 - 400)/100,\ x_2 = (X_2 - 1.35)/0.48,$$
$$x_3 = (X_3 - 3)/1\ \&\ x_4 = (X_4 - 3)/1 \quad \ldots (6)$$

Results and Discussion

Estimated regression coefficient for response and analysis of variance (ANOVA)

The coefficients of the polynomial model (see Eq. 2), T- values, P-values, and the standard error (SE) of the coefficient were shown in Table 3, where the SE of the coefficient is a measure of the variation in estimating the coefficient. The ratio of the coefficient to the standard error can be characterized by T-value. The importance of the coefficients of the polynomial model was determined by T-values and P-values, where the larger the magnitude of T-value and the smaller the P-value indicate the considerable importance of the corresponding coefficient[20]. The results of the quadratic and linearity model in the form of ANOVA showed a small probability value ($P < 0.05$), indicating that the individual terms in the model have a significant effect**.**

The model equation for the mixing time obtained after performing 30 experiments with a 96% confidence is as follows:

$$\hat{Y}_i = 6.5833 - 3.45833x_1 - 0.7333x_3 + 1.775x_i^2 + 1.0258x_2^2 + 1.5625x_3^2 + 2.2x_4^2 \quad \ldots (7)$$

The predicted values and experimental results obtained by the model equation (see Eq. 7) are given in Table 3.

Optimization of model

The second-order models include the critical points such as maximum, minimum, saddle, and ridge. The stationary point can be found by solving matrix algebra. The fitted second-order model in matrix form is as follows[11]:

$$\hat{Y} = \hat{\beta} + xb + Bx^2 \quad \ldots (8)$$

The derivative of $\hat{Y}$ with respect to the elements of the vector x is

Table 2 — Parameter levels of CCRD (coded value) and the results experimental and predicted values for mixing time.

Run order	Block	x_1	x_2	x_3	x_4	Mixing time (s)	
						Experimental	Predicted
1	1	1	1	1	1	10	9.56
2	1	1	1	1	-1	9.2	8.40
3	1	1	1	-1	1	11	10.15
4	1	1	1	-1	-1	10.3	9.36
5	1	1	-1	1	1	9.5	9.45
6	1	1	-1	1	-1	9	9.05
7	1	1	-1	-1	1	11.5	10.80
8	1	1	-1	-1	-1	11.8	10.74
9	1	-1	1	1	1	15.5	15.25
10	1	-1	1	1	-1	16.8	16.55
11	1	-1	1	-1	1	17.5	16.50
12	1	-1	1	-1	-1	19.4	18.140
13	1	-1	-1	1	1	14.5	14.50
14	1	-1	-1	1	-1	17	16.54
15	1	-1	-1	-1	1	17	16.49
16	1	-1	-1	-1	-1	19.4	18.88
17	1	2	0	0	0	5.5	6.77
18	1	-2	0	0	0	19.6	20.60
19	1	0	2	0	0	8.6	10.37
20	1	0	-2	0	0	10.5	11.00
21	1	0	0	2	0	11.4	11.37
22	1	0	0	-2	0	12	14.30
23	1	0	0	0	2	14	14.77
24	1	0	0	0	-2	14.5	16.00
25	1	0	0	0	0	7	6.58
26	1	0	0	0	0	6.50	6.58
27	1	0	0	0	0	6.50	6.58
28	1	0	0	0	0	6	6.58
29	1	0	0	0	0	6.50	6.58
30	1	0	0	0	0	7	6.58

Table 3 — Results of the regression analysis of the CCRD

Term	Coef	SE Coef	T-value	P-value
Constant	6.58333	0.4985	13.206	0.000
x_1	-3.45833	0.2493	-13.874	0.000
x_2	-0.15833	0.2493	-0.635	0.535
x_3	-0.73333	0.2493	-2.942	0.010
x_4	-0.30833	0.2493	-1.237	0.235
x_1*x_1	1.77500	0.2332	7.613	0.000
x_2*x_2	1.02500	0.2332	4.396	0.001
x_3*x_3	1.56250	0.2332	6.701	0.000
x_4*x_4	2.20000	0.2332	9.435	0.000
x_1*x_2	-0.16250	0.3053	-0.532	0.602
x_1*x_3	0.16250	0.3053	0.532	0.602
x_1*x_4	0.61250	0.3053	2.006	0.063
x_2*x_3	0.18750	0.3053	0.614	0.548
x_2*x_4	0.18750	0.3053	0.614	0.548
x_3*x_4	0.08750	0.3053	0.287	0.778

$$\partial \hat{Y} / \partial x = b + 2Bx = 0 \quad \ldots (9)$$

Therefore, the solution to the stationary point is:

$$x_S = -\frac{1}{2} B^{-1} b \quad \ldots (10)$$

where $b = \begin{bmatrix} \hat{\beta}_1 \\ \hat{\beta}_2 \\ \vdots \\ \hat{\beta}_q \end{bmatrix}$ and $B = \begin{bmatrix} \hat{\beta}_{11}, \hat{\beta}_{12}/2, \ldots, \hat{\beta}_{1q}/2 \\ \hat{\beta}_{21}/2, \hat{\beta}_{22}, \ldots \hat{\beta}_{2q}/2 \\ \vdots \qquad\qquad \vdots \\ sym. \qquad\qquad , \hat{\beta}_{qq}/2 \end{bmatrix}$

As a result, the optimum response value can be calculated as:

$$\hat{Y}_S = \hat{\beta}_0 + \frac{1}{2} x_S' b \quad \ldots (11)$$

Optimum response values from the model are shown in Table 4. According to the experimental design for the tracer injection points and also the probe location, it is obvious that the optimum points are located in zone 3 as illustrated in Table 4. These zones are situated in the opposite direction to each other. This is due to the probe location and the tracer injection point, both of which are located in the middle of two impellers, where the liquid velocity in this region is quite high, and the tracer can be quickly dispersed to the other region. So by keeping these two parameters constant during the next experiments, the impeller rotational speed and rate of aeration for both configurations was investigated.

Comparison of mixing times

The reasons for the different measurement mixing times are due to differences in operating condition, geometries of the mixing system, measurement techniques and experimental procedures such as location of the injection point, probe location, vessel size, impeller clearance, etc[21]. Paglianti and Pintus[7] compared mixing time using two methods (conductivity technique and decolorization) and showed that the predicted mixing time can be different between these two techniques. Bujalski *et al.*[22] successfully simulated the effect of the radial distance of the tracer addition point at liquid surface on mixing time using CFD with a sliding mesh approach, and showed that the injection point significantly influenced mixing time.

Table 4 — Response optimization of the nonlinear polynomial model

Variables	Optimum (Coded value) value(coded)	Optimum (Real value) value(uncoded)
Probe location	0.2347	3.23≈ 3
Tracer injection point	0	3

Table 5 — Comparison of the mixing time obtained from the experimental and simulation values

	$N.t_{95\%}$	% Deviation
Present study (single Rushton impeller)	42	
S.L.Yeoh *et al.*[21] (CFD)	33.2	+26.5
H. Hartmann *et al.*[24] (CFD)	54.7	-23.2
Wang Zheng *et al.*[25] (CFD)	66.5	−36.84
Sano and Usui[26]	47	−10.64
Shiue and Wong[27]	70	-40
Fasano and Penney[28]	30.7	+36.8
M. Lunden *et al.*[34]	51	-17.65

Magelli *et al.*[23] investigated that the mixing time is affected in number of different geometrical configurations and sizes of the stirred vessels, impeller types. Also, effect of probe location[4], location of injection point in various diameters of the impeller[24] and probe location and injection point at different impeller speeds[25] on the experimentally measured mixing time has been investigated.

In the present study the obtained mixing time was compared against simulation results and published data based on experimental works for a Rushton impeller in different configurations of a vessel (see Table 5).

The best agreement (10.64%) was found with the result in literature[26]. The maximum deviations are 40%, 36.84% and 36.8% from the measured values of Shiue and Wong[27], Fasano and Penney[28] and Zheng *et al.*[25] respectively

Effect of impeller rotational speed

Figure 2 shows that for both systems, mixing time decreases because the turbulent intensity and the liquid circulation speed were increased with an increase in impeller speed. Zhang *et al.*[29] have made similar observations for the single impeller systems.

At high impeller rotational speed, the variation of mixing time is slight. The experimental single phase mixing times obtained for single and dual Rushton turbine stirred tank were compared with values from Lu[30] in Fig. 2.

The measured mixing times for a single Rushton impeller in Fig. 2 showed little deviation with values from Lu[30], which is due to the high bottom clearance (C=T/2) in this system.

In the turbulent region (Re>10000) the dimensionless mixing time, $N.t_m$ will remain constant and the dimensionless mixing time is independent of Reynolds number in turbulent flow while other design and operation factors are held fixed. According to the experimental results, the dimensionless mixing times for single and dual Rushton impeller stirred tanks are 42 and 41.5 respectively, and are approximately equal. Lu[30] obtained the following correlation by correlating the mixing time with n_b, B/T, Q_g and N, for gas-liquid system equipped with a single Rushton turbine impeller[30].

$$t_m = 55.7 \times n_b^{-0.3} \left(\frac{B}{T}\right)^{-0.1535} \times \left(\frac{Q_g}{N^2 D^3}\right)^{0.0296} \quad \ldots (13)$$

A comparison between the predicted values from Eq. 13 and the experimental values of the gas-liquid mixing time is shown in Fig. 3. It can be seen that the experimental results for Re>50000 are also in good agreement with the correlation data. As shown in Figs. 2 and 3, the experimental results for single Rushton impeller agree well with dual Rushton impeller stirred tank.

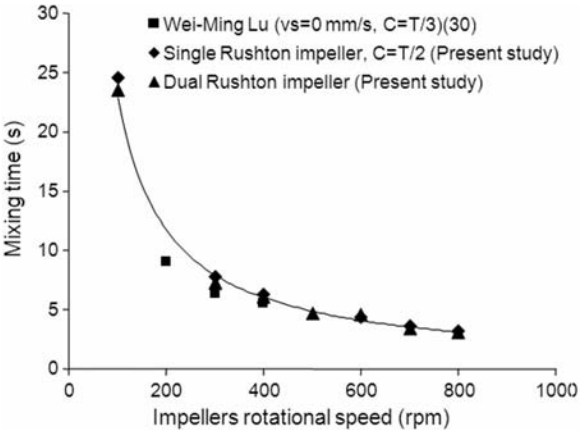

Fig. 2 — Effect of impeller rotational speed on mixing time under non-aerated systems

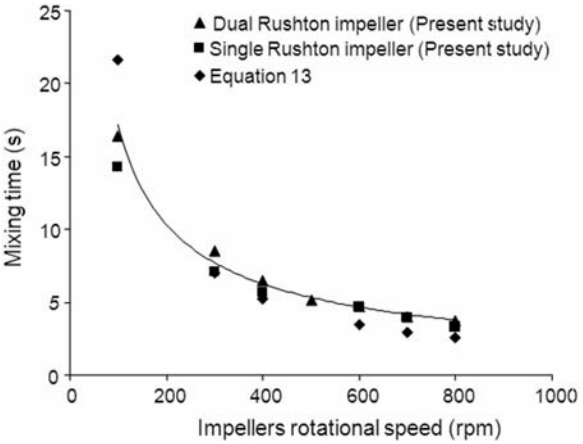

Fig. 3 — Effect of impellers rotational speed on mixing time under aerated systems (vs=3.14 mm/s).

Effect of aeration

In gas-liquid stirred tank besides the axial turbulent liquid exchange and circulation flow, induced flow during aeration is found as a consequence of the density difference. According to Eq. 14, this flow is dependent on the gas flow rate and pumping capacity, which is identified with gas induced at axial flow rate[31,32].

$$Q_{IF} = K \frac{Q_g}{\frac{P_g}{P_U} ND^3} \quad \ldots (14)$$

In gas-liquid agitated vessel, the mixing time was affected by gas flow rate. In the previous literature reviews, there are many contradictions to the effect of the gas flow rate on the mixing time. An increase in gas flow rate can increase, decrease, or have no effect on the mixing time[29]. Zhang *et al.*[29] studied the mixing behaviour in a stirred tank with a single Rushton turbine impeller and found that the mixing time increased when the gas flow rate increased at constant impeller speed.

Shewale and Pandit[33] also investigated the effect of gas flow rate on mixing time; they found the mixing time decreased when the gas flow rate increased. So that, the different effect of aeration on the mixing time was found. The effects of the superficial gas velocity on mixing time investigated in this work are shown in Figs. 4a and 4b.

The created turbulency in two phase mixing system depends on both of the impeller speed and aeration.

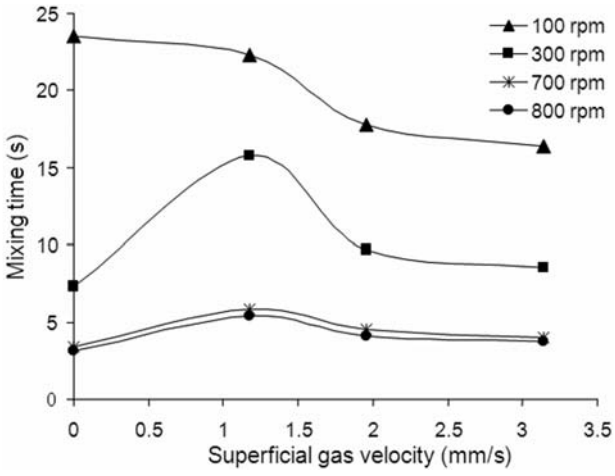

Fig. 4a — Effect of superficial gas velocity on mixing time for dual impeller system.

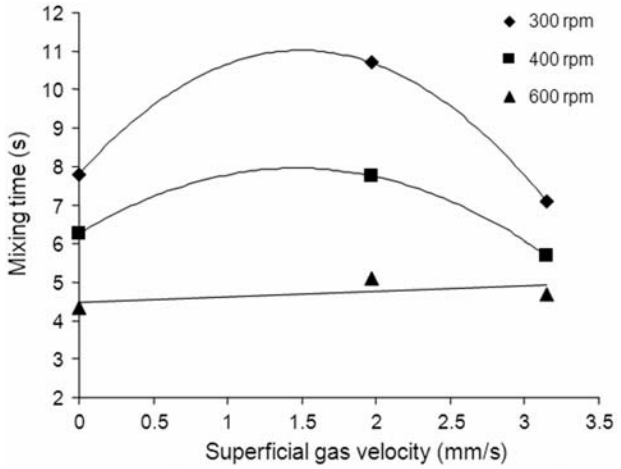

Fig. 4b — Effect of superficial gas velocity on mixing time for single impeller system.

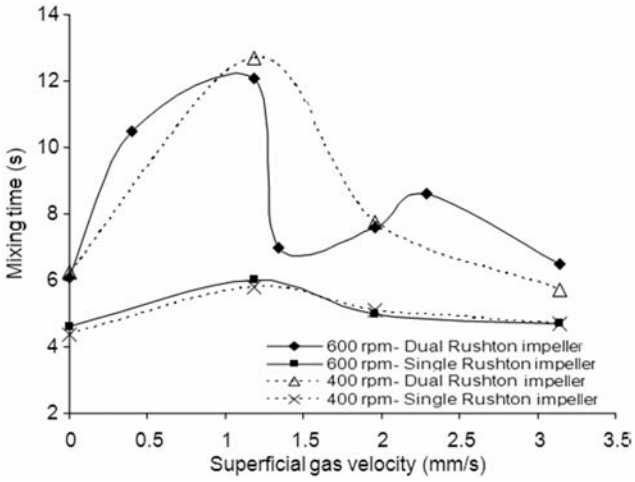

Fig. 5 — Comparison between two mixing systems.

Further more, for expressing the effect of gas phase on the mixing time, it's essential to investigate the interaction between gas flow rate and impeller speed in different flow regimes (flooding and loading).

From Fig. 4, it is obvious that increasing the superficial gas velocity in the low rotational speed of impellers increases pneumatical agitation power, consequently the mixing time decreased. Again by increasing the superficial gas velocity (v_s) from 0 to 1.3 mm/s at 300 and 400 the rotational speed of the impeller mixing times for both systems rise, while for the rates between 1.3 -3.14 mm/s there is a downward trend. When N≥ 600 rpm the value of the mixing time leveled off with an increase in the superficial gas velocity. Further, the value of the superficial gas velocity did not affect the value of the mixing time, since the influence of the impeller rotation at high speed is higher than the superficial gas velocity. In higher than 600 rpm, decreasing the mechanical agitated power, increases the mixing time; but increasing the pneumatical agitation power decrease the mixing time in this state. Therefore, the mixing time doesn't change significantly due to simultaneous interaction of these effects. Also, at high superficial gas velocities the changes in mixing time in all rotational speeds will remain approximately constant. This may be because the impeller pumped a considerable amount of fluid in the radial direction. So, it can be said the impeller is flooded. As shown in Fig. 4a, the mixing time of the gas–liquid phase in dual Rushton impeller tank was higher than that of the single phase. This is because the impeller pumping capacities in gas-liquid mixing system are less than the single phase.

By increasing the superficial gas velocity from 0 - 1.3 mm/s, the mixing time increases because of the drop in mechanical power due to reduced pumping capacity. In fact, within this range of aeration rate, the induced flow cannot remedy this power loss. When $v_s \geq$ 1.3 mm/s, the pneumatical agitation power dominate and mixing time decreases.

Figure 5 shows the general comparison between two mixing systems. It is completely obvious that mixing times are approximately equal for both systems. Consequently, with having mixing times constant in the same geometry for both systems, an optimized liquid level for dual Rushton impeller stirred tank has been achieved in our study.

To have mixing times fixed after adding a top impeller to a single Rushton impeller stirred tank, the liquid level into the second system should be adjusted 1.8 times its corresponding value for the first system. When the liquid level of the second system is not equal with this size, the mixing time and uniformity might be affected. Therefore, the correlation of liquid level in multi-impeller agitated tanks, with n and T took the following form:

$$\frac{H_D}{T} = 1.8(n-1) \quad n \geq 2 \qquad \ldots (15)$$

where n and H_D are the number of impellers and liquid level in dual impeller agitated tanks respectively.

Conclusion

In this paper, by Response Surface Methodology the optimum position for injection tracer and probe location in a dual-Rushton stirred tank has been investigated. According to the experimental design for tracer injection points and also probe location, it can

be assumed that the optimum points for both parameters are opposed at the entrance of the tank (point 3). Effects of superficial gas velocity and impeller rotational speed for both systems are investigated. Mixing time decreases with an increase in impeller speed. When N≥700rpm, the value of mixing time leveled off with the increasing impeller rotational speed. It can be seen from the results that by increasing the superficial gas velocity, the mixing time at the low rotational speed (100 rpm) decreases; however, the reduction of mixing time at the higher rotational speed would be from 1.3 mm/s of superficial gas velocity, while for less than the mentioned superficial gas velocity the reverse effect is seen. When N≥ 600 rpm, the value of the mixing time leveled off with the increasing superficial gas velocity, and the value of the superficial gas velocity did not affect the value of the mixing time. According to the experimental results, the dimensionless mixing times for single and dual Rushton impeller stirred tanks are 42 and 41.5 respectively. Consequently, mixing times are equal for both systems. An effective circulation loop and optimum mixing time can be achieved with an optimized liquid level in a dual Rushton impeller tank that equals H_D = 1.8T.

Nomenclature

N	impeller rotational speed	[rpm]
v_s	superficial gas velocity	[mm/s]
Y	response variable	[-]
x	coded variable level	[-]
T	tank diameter	[m]
D	impeller diameter	[m]
H_D	height of the liquid in the multi-impellers tank	[m]
ΔC	impeller spacing	[m]
C	off bottom clearance of the lower turbine	[m]
C(t)	tracer concentration at time t	[Kg/m^3]
σ^2	dimensionless variance	[-]
t_m	mixing time	[s]
n_b	baffle number	[-]
B	baffle width	[m]
P_g	power consumption with aeration	[W]
P_U	power consumption without aeration	[W]
n	number of impeller	[-]
L	impeller blade width	[m]
W	impeller blade height	[m]

References

1 You S T, Abdul Raman A A, Raja Ehsan Shah R S S & Mohamad Nor M I, *Rev Chem Eng*, 30 (3) (2014) 323.
2 Zadghaffari R, Moghaddas J S & Revstedt J, *Indian J Chem Eng*, 5 (2008) 13.
3 Broniarz Press L, Woziwodzki S & Ochowiak M, *Proceedings of European Congress of Chemical Engineering* (Copenhagen), 2007.
4 Houcine I, Plasari E & David R, *Chem Eng Technol*, 23 (2000) 605.
5 Manna L, *Chem Eng J*, 67(3) (1997) 167.
6 Chomcharn N, *Biological Pharmaceutical Engineering,* M S Thesis, Otto H York Department of Chemical, 2009.
7 Paglianti A & Pintus S, *Exp Fluids*, 31 (2001) 417.
8 Otomo N, Bujalski W & Nienow A W, *Process Inst Chem Eng Res Event*, (1995) 829.
9 Pandit A B & Joshi J B, *Chem Eng Sci*, 38 (1983) 1189.
10 Ochieng A, Onyango M S, *Chem Eng Process*, 47 (2008) 1853.
11 Bradley N, *The response surface methodology*, PhD Thesis, Indiana University South Bend, 2007.
12 Das S R, Dhupal D & Kumar A, *IJAE*, 3 (2013) 284.
13 Kwak J S, *Int J Mach Tools Mfr*, 45 (2005) 327.
14 Aslan N, *Fuel*, 86 (2007) 769.
15 Tanyildizi M S, Özer D & Elibol M, *Process Biochem*, 40 (2005) 2291.
16 Kresta S M & Mao D, *Chem Eng Sci*, 61 (2006) 2823.
17 Paul E L, Atiemo Obeng V A & Kresta S M, *Handbook of Industrial Mixing: Science and Practice* (Wiley-IEEE, I Chem E, Rugby), 2004 283.
18 Ruszkowski S, *Proceedings of 8th European Mixing Conference* (Cambridge, UK), 1994.
19 Açikalin K, Karaca F & Bolat, E, *Fuel Process Technol*, 87 (2005) 17.
20 Thakkar A & Saraf M, *Nat Prod Bioprospect*, 4(6) (2014) 341.
21 Yeoh S L, Papadakis G & Yianneskis M, *Chem Eng Sci*, 60 (2005) 2293.
22 Bujalski J M, Jaworski Z, Bujalski W & Nienow A W, *Chem Eng Res Des*, 80 (2002) 824.
23 Magelli F, Montante G, Pinelli D & Paglianti A, *Chem Eng Sci*, 101 (2013) 712.
24 Hartmann H, Derksen J J & Van den Akker H E A, *A I Ch E J*, 52 (2006) 3696.
25 Zheng W, Zai-sha M A O & Xian-qian S, *Chin J Process Eng*, 6 (2006) 857.
26 Sano Y & Usui H, *J Chem Eng Jpn*, 18 (1985) 47.
27 Shiue S J & Wong C W, *Can J Chem Eng*, 62 (1984) 602.
28 Fasano J B & Penney W R, *Chem Eng Prog*, 87 (1991) 56.
29 Zhang Q, Yong Y, Mao ZS, Yang C & Zhao C, *Chem Eng Sci*, 64 (2009) 2926.
30 Lu W M, Wu H Z & Ju M Y, *Chem Eng Sci*, 52 (1997) 3843.
31 Vasconcelos J M T, Alves S S, Nienow A W & Bujalski W, *Can J Chem Eng*, 76 (2009) 398.
32 Vrabel P, Van Der Lans R, Cui Y Q, Luyben K & Ch A M, *Chem Eng Res Des*, 77 (1999) 291.
33 Shewale S D & Pandit A B, *Chem Eng Sci*, 61 (2006) 489.
34 Lunden M, Stenberg O & Andersson B, *Chem Eng Commun*, 139 (1995) 115.